Reaction Force Analysis of Solvent Effects in the Addition of HCl to Propene

Jaroslav V. Burda,[†] **Jane S. Murray,*[,‡,§] Alejandro Toro-Labbé,**[||] **Soledad Gutiérrez-Oliva,**[||] **and Peter Politzer**[‡,§]

Department of Chemical Physics and Optics, Faculty of Mathematics and Physics, Charles University, Ke Karlovu 3, 112 16 Prague, Czech Republic, Department of Chemistry, Cleveland State University, Cleveland, Ohio 44115, Department of Chemistry, University of New Orleans, New Orleans, Louisiana 70148, and Laboratorio de Química Teórica Computacional (QTC), Facultad de Química, Pontificia Universidad Católica de Chile, Vicuña Mackenna 4860, Casilla 306, Correo 22, Santiago, Chile

We have investigated computationally, via reaction force analyses, the addition of HCl to propene, both Markovnikov and anti-Markovnikov, in the gas phase and in chloroform solution. The calculations were carried out at the CCSD(T)/aug-pVTZ//B3LYP/aug-cc-pVDZ level. A particular interest was in the magnitudes of the two components of the activation energies that are defined by the minimum of the reaction force for each process. The total activation energies for Markovnikov and anti-Markovnikov addition are found to be, respectively, 39.7 and 45.9 kcal/mol in the gas phase and 27.1 and 34.9 kcal/mol in chloroform solution. In solution, the first portion of the reaction (prior to the reaction force minimum) involves substantial stretching of the H–Cl bond, which makes that contribution to the total activation energy greater than in the gas phase. However the second part of the activation is much less energy demanding in solution for both the Markovnikov and anti-Markovnikov additions. The overall preference for Markovnikov addition is due to the electrostatic potential of propene favoring the initial approach of the HCl hydrogen to the terminal carbon.

1. The Reaction Force

The reaction force $\mathbf{F}(\mathbf{R})$ is defined classically,[1] as the negative gradient of the potential energy $V(\mathbf{R})$ of a chemical or physical process along a reaction coordinate $\mathbf{R}$:

$$\mathbf{F}(\mathbf{R}) = -\frac{\partial V(\mathbf{R})}{\partial \mathbf{R}} \qquad (1)$$

$\mathbf{R}$ is normally taken to be the intrinsic reaction coordinate.[2,3]

Figure 1 shows a typical $V(\mathbf{R})$ profile and the corresponding $\mathbf{F}(\mathbf{R})$ for a process involving a single energy barrier in the forward and reverse directions; whether exothermic or endothermic is immaterial to this discussion. $\mathbf{F}(\mathbf{R})$ has a minimum and a maximum at the inflection points of $V(\mathbf{R})$, $\mathbf{R} = \alpha$ and $\mathbf{R} = \gamma$. These points divide the process into three regions: reactants $\rightarrow \alpha$, $\alpha \rightarrow \gamma$, and $\gamma \rightarrow$ products. In studies involving a variety of reactions—proton transfers, molecular rearrangements, conformational changes, S_N2 substitution, bond dissociation/formation—we have found that these regions have certain characteristic features. (For reviews, see Politzer et al.,[4] and Toro-Labbé et al.[5,6])

In going from the reactants to α, structural changes are dominant: bond stretching, angle bending, rotations, etc. These prepare the reactants for subsequent steps, but they are resisted by an increasingly negative (retarding) reaction force $\mathbf{F}(\mathbf{R})$, which reaches its greatest magnitude at α. At this point, the system can be described as activated forms of the reactants.

Between α and γ is the transition-to-products region. Although structural factors are still important, it is here that significant electronic effects are most likely to take place: bond
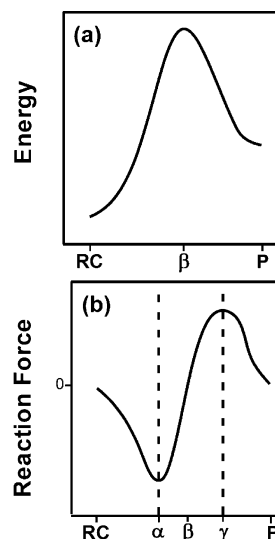

Figure 1. Characteristic profiles of the potential energy (a) $V(\mathbf{R})$ and the reaction force (b) $\mathbf{F}(\mathbf{R})$ along the intrinsic reaction coordinate $\mathbf{R}$ for a process having an activation barrier in both directions. The points $\mathbf{R} = \alpha$ and $\mathbf{R} = \gamma$ correspond to the minimum and the maximum of $\mathbf{F}(\mathbf{R})$; the transition state is at $\mathbf{R} = \beta$. The zero of $\mathbf{F}(\mathbf{R})$ is indicated.

breaking and formation, rapid and extensive variations in properties such as orbital energies and electrostatic potentials, etc. All this is accompanied by a positive and increasing driving force that counters and then balances the retarding one, at $\mathbf{R} = \beta$, corresponding to the maximum of $V(\mathbf{R})$. $\mathbf{F}(\mathbf{R})$ reaches its strongest positive value at γ, which marks the end of the transition region; the system can now be viewed as being in activated states of the products. The region after γ is again structurally dominated, as these relax to their final forms.

Note that since the three regions are established by the extrema of $\mathbf{F}(\mathbf{R})$, they are a natural and rigorous consequence

* Corresponding author. E-mail: jsmurray@uno.edu.
† Charles University.
‡ Cleveland State University.
§ University of New Orleans.
|| Pontificia Universidad Católica de Chile.

(via eq 1) of the specific form of V($\mathbf{R}$). For the reverse reaction, the coordinate $\mathbf{R}$ is in the opposite direction and $\mathbf{F}(\mathbf{R})$ is the negative (mirror image) of Figure 1b.

An interesting point that emerges from the reaction force analysis is its focus upon a transition region, rather than the single state corresponding to the maximum of V($\mathbf{R}$) at $\mathbf{R} = \beta$. Consistent with this is the fact that the position-dependent reaction force constant $\kappa(\mathbf{R})$, the second derivative of V($\mathbf{R}$), is negative throughout the entire region between α and γ.[7,8]

Further support comes from studies of specific reactions. In an intramolecular proton transfer, the calculated force constant for movement along the reaction coordinate was found to be negative from the $\mathbf{F}(\mathbf{R})$ minimum to its maximum.[7] Also, for a series of diatomic molecular dissociations, bond-stretching force constants, both experimentally based[9] and computed,[10] became negative very close to the respective $\mathbf{F}(\mathbf{R})$ minima and remained negative as the atoms separated thereafter.

Particularly significant is that a similar conclusion has been reached from transition state spectroscopy, as recently pointed out.[8] In this area, the term "transition state" has come to be applied to the whole sequence of transient configurations through which a system passes in going from perturbed forms of the reactants to perturbed forms of the products.[11-13] This is accordingly a transition region, not a state, the same concept that emerges from $\mathbf{F}(\mathbf{R})$ and $\kappa(\mathbf{R})$ analyses, which also establish its boundaries.

An aspect of the reaction force that plays an important role in the work being presented is its natural decomposition of an activation energy into two components

$$\begin{aligned}\Delta E_{act} &= V(\beta) - V(\text{reactants}) \\ &= [V(\beta) - V(\alpha)] + [V(\alpha) - V(\text{reactants})] \\ &= \Delta E_{act,2} + \Delta E_{act,1}\end{aligned}$$

(2)

$\Delta E_{act,1}$ is the energy needed to go from the reactants to α, primarily to overcome resistance to the structural changes taking place. $\Delta E_{act,2}$ is the energy requirement for the initial portion of the transition to products, $\alpha \rightarrow \beta$.

Determining these separate contributions to ΔE_{act} can provide important insight into the activation process.[5,6,14] It can also help to elucidate the effect of an external agent (e.g., a solvent, catalyst, electric field, etc.), by showing whether the latter influences more the structurally or electronically related component of the activation energy. This has been demonstrated for an S_N2 substitution in aqueous solution[14] and for the keto−enol tautomerization of thymine in the presence of Mg(II) ion.[5,6]

2. Addition of HCl to Propene: Procedure and Results

In the present work, we have addressed an addition process, HCl adding to the double bond of propene, $H_2C_a=C_bH-CH_3$, both in the gas phase and in chloroform solution. This follows Markovnikov's rule, and yields $H_3C_a-C_bHCl-CH_3$.[15] However we have also looked at the formation of the anti-Markovnikov product, $C_aH_2Cl-C_bH_2-CH_3$. The geometries of the system along the intrinsic reaction coordinate were optimized at the density functional B3LYP/aug-cc-pVDZ level, followed by single-point CCSD(T)/aug-pVTZ energy calculations to give the respective V($\mathbf{R}$), from which were obtained the $\mathbf{F}(\mathbf{R})$ via eq 1.

The effect of the solvent was included by means of the COSMO continuum approach,[16,17] using a dielectric constant of 4.90 for chloroform. Because the intrinsic reaction coordinate in solution may differ from that in the gas phase, they were

TABLE 1: Optimized Interatomic Distances and Angles (Å and deg)[a]

distance or angle	RC	α	β	γ	P
Gas Phase					
Markovnikov					
H_a-Cl	1.312	1.315	1.885	2.532	2.974
C_a-H_a	2.341	1.798	1.226	1.094	1.099
C_b-Cl	3.717	2.835	2.746	2.434	1.847
C_a-C_b	1.341	1.343	1.412	1.500	1.521
$\angle H_a-C_a-C_b$	79	76	86	109	111
$\angle Cl-C_b-C_a$	76	87	86	96	109
$\angle H-C_a-C_b$	122	121	118	112	111
	121	121	118	109	109
$\angle H-C_b-C_a$	118	119	118	117	110
$\angle C-C-C$	125	125	124	120	114
Anti-Markovnikov					
H_a-Cl	1.312	1.390	1.889	2.497	2.961
C_b-H_a	2.463	1.729	1.256	1.096	1.100
C_a-Cl	3.638	2.630	2.608	2.364	1.831
C_a-C_b	1.341	1.355	1.402	1.497	1.521
$\angle H_a-C_b-C_a$	69	66	76	103	109
$\angle Cl-C_a-C_b$	83	96	94	99	112
$\angle H-C_a-C_b$	122	122	122	121	112
	121	122	122	118	112
$\angle H-C_b-C_a$	118	118	116	110	106
$\angle C-C-C$	125	123	122	119	115

distance or angle	RC	α	β	γ	P
Chloroform Solution					
Markovnikov					
H_a-Cl	1.323	1.600	2.143	2.811	2.930
C_a-H_a	2.217	1.582	1.168	1.093	1.096
C_b-Cl	3.642	3.109	3.053	2.345	1.867
C_a-C_b	1.343	1.365	1.418	1.503	1.519
$\angle H_a-C_a-C_b$	80	76	90	112	111
$\angle Cl-C_b-C_a$	74	80	83	105	109
$\angle H-C_a-C_b$	121	120	116	109	109
	121	120	117	111	111
$\angle H-C_b-C_a$	118	118	118	116	111
$\angle C-C-C$	125	126	125	117	114
Anti-Markovnikov					
H_a-Cl	1.322	1.790	2.236	2.853	2.967
C_b-H_a	2.376	1.603	1.214	1.100	1.100
C_a-Cl	3.516	2.760	2.746	2.367	1.846
C_a-C_b	1.343	1.371	1.401	1.497	1.519
$\angle H_a-C_b-C_a$	67	54	72	106	109
$\angle Cl-C_a-C_b$	84	105	103	108	112
$\angle H-C_a-C_b$	122	121	122	120	112
	121	121	121	118	112
$\angle H-C_b-C_a$	119	118	116	107	106
$\angle C-C-C$	125	124	123	119	115

[a] RC = reactant complex, P = product.

determined separately. The use of a continuum model for solvation assumes that the solvent is at all times equilibrated to the solute.[18,19] This is most questionable in the vicinity of the transition state because of its short lifetime; however, the resulting underestimation of the activation energy is usually relatively minor.[19] It can be important for very fast processes, e.g., electron transfer, for which a nonequilibrium solvation treatment is needed.[20]

All ΔE values are from energy minima at 0 K. Both in the gas phase and in solution, the reaction coordinate $\mathbf{R}$ for the addition begins with a weakly bound reactant complex (RC) in which the HCl hydrogen is interacting with the π electrons of the propene double bond. The complex RC is lower in energy than the free reactants by 4.0 kcal/mol in the gas phase and 2.6 kcal/mol in solution.

TABLE 2: Computed Components of ΔE for Markovnikov and Anti-Markovnikov Additions of HCl to $H_2C=CH-CH_3$, Gas Phase and in Chloroform Solution[a]

process	ΔE (RC→α)	ΔE (α→β)	$\Delta E_{act,f}$	ΔE (β→γ)	ΔE (γ→P)	$\Delta E_{act,r}$	$\Delta E_{overall}$
			Gas Phase				
Markovnikov	10.5	29.2	39.7	−24.4	−33.5	57.8	−18.1
anti-Markovnikov	25.4	20.5	45.9	−26.9	−34.3	61.2	−15.3
			Chloroform Solution				
Markovnikov	16.1	11.0	27.1	−20.9	−24.6	45.5	−18.4
anti-Markovnikov	26.5	8.4	34.9	−20.9	−29.5	50.3	−15.5

[a] RC = reactant complex, P = product. All ΔE are in kcal/mol and are for the forward reaction, except for $\Delta E_{act,r}$.
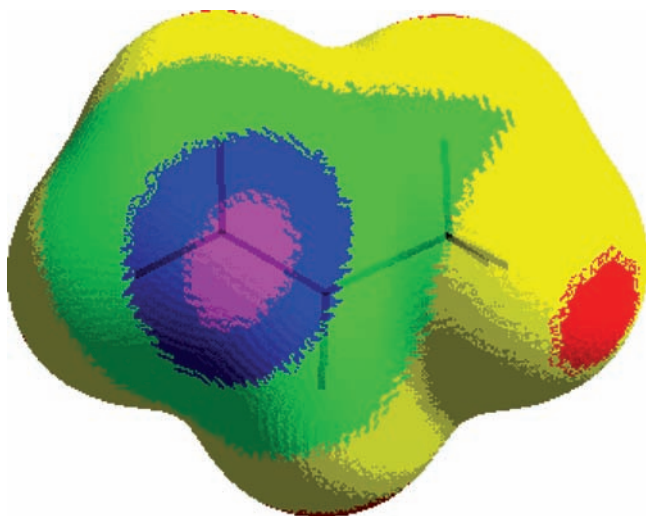

Figure 2. Calculated electrostatic potential on the 0.001 au molecular surface of propene. Color ranges, in kcal/mol, are: purple, more negative than −15; blue, between −15 and −10; green, between −10 and 0; yellow, between 0 and 8; red, greater than 8. The methyl group is at the right. The most negative region (purple) is above and below the C=C double bond, but can be seen to be shifted toward the terminal carbon (at the left).

In Table 1 are summarized optimized bond lengths and bond angles for each of the four processes at five points along **R**: RC (reactant complex), α, β, γ, and P (product). In Table 2 are the changes in the energy of the system between these five points as well as the forward and reverse activation barriers and the overall ΔE.

Because the addition of HCl to propene is electrophilic,[15] we obtained additional perspective by computing the electrostatic potential (B3LYP/6-31G**) on the molecular surface of propene, taking this to be the 0.001 au contour of its electronic density.[21] The most negative potentials are above and below the C_a-C_b double bond, with minima of −16 kcal/mol (Figure 2); these are shifted somewhat toward the terminal carbon, C_a.

3. Addition of HCl to Propene: Discussion

In all four processes (Markovnikov and anti-Markovnikov, gas phase and solution), the initial approach of the HCl is with its hydrogen, H_a, pointing toward one of the negative potentials of the double bond. During the first part of the reaction, before the $F(R)$ minimum at α, the HCl realigns itself so that H_a points toward the carbon to which it will later bond. In the presence of the solvent, this is accompanied by a considerable stretching of the H_a-Cl bond.

In the α → γ transition region of the reaction, between the minimum and maximum of $F(R)$, H_a breaks away from the chlorine and forms a C_a-H_a (Markovnikov) or C_b-H_a (anti-Markovnikov) bond. By the point $R = \gamma$, these have essentially their final equilibrium C−H bond lengths. Meanwhile, the chlorine has been approaching and interacting with the other carbon (especially between β and γ) while the latter reconfigures from trigonal to tetrahedral and the C_a-C_b bond lengthens. At each $F(R)$ maximum ($R = \gamma$), we have essentially a 2-chloropropane (Markovnikov) or a 1-chloropropane (anti-Markovnikov) molecule with a highly stretched C−Cl bond. In the last part of each process, these molecules relax to their final forms.

In the gas phase, Table 2 shows that the overall CCSD(T) ΔE for the Markovnikov addition (relative to RC) is −18.1 kcal/mol; for the anti-Markovnikov, it is −15.3 kcal/mol. These values are predicted to change only slightly in the chloroform solution, to −18.4 and −15.5 kcal/mol. When B3LYP/6-31G** zero-point and thermal contributions are added to the gas phase ΔE, we obtain ΔH(298 K) of −17.9 kcal/mol (Markovnikov) and −14.8 kcal/mol (anti-Markovnikov); both are relative to the free reactants. These are in excellent agreement with the results from experimental gas phase heats of formation,[22] −17.3 and −14.2 kcal/mol, respectively.

We are interested particularly in the activation energies and their components as established by the $F(R)$ minima, eq 2. As anticipated, the total activation energy is less for Markovnikov addition than for anti-Markovnikov, both in the gas phase and in solution (Table 2). In the gas phase, the values are 39.7 and 45.9 kcal/mol; the chloroform solvent lowers both quite substantially, to 27.1 and 34.9 kcal/mol.

The components of ΔE_{act} give us a more detailed picture (Table 2). As mentioned above, all four processes begin (RC → α) with the alignment of the HCl so that its hydrogen points toward the carbon with which it will bond. In the gas phase, this is facilitated for Markovnikov addition by the electrostatic potential of propene favoring C_a; for anti-Markovnikov, this electrostatic factor must be overcome. This contributes to the 15 kcal/mol increase in ΔE (RC → α). In solution, the HCl realignment is accompanied by stretching the H_a-Cl bond, which increases ΔE (RC → α), but the electrostatic effect is again evident.

In the second portions of the activations, α → β, the reactions in solution are greatly favored, requiring much less energy. The major events between α and β are the continued breaking of the H_a-Cl bond and the formation of the H_a-C, and the bond lengths in Table 1 show that the processes in solution are more advanced in both respects at $R = \alpha$ than are those in the gas phase.

The reverse reactions can be analyzed in the same manner, using the data in Tables 1 and 2. In each instance, the stretching of the C−Cl bond dominates the first portion of the activation, and this is helped by the presence of the solvent.

In our two earlier studies of the effects of external agents upon activation processes,[5,6,14] their influence in diminishing the activation energy was primarily in the initial regions, before the $F(R)$ minima, which are characterized largely by structural

Reaction Force Analysis of Solvent Effects

J. Phys. Chem. A, Vol. 113, No. 23, 2009 **6503**

changes, which the agent facilitated. In the addition of HCl to propene, however, the chloroform solvent actually increases the energy needs in the **R** → α regions because it induces, presumably by its polarity, the stretching of the H_a–Cl bond. It is between α and β that the rate enhancement by the solvent occurs.

Finally, Table 2 shows that the preference for Markovnikov addition is established in the first part of the activation, before the **F**(**R**) minimum, both in the gas phase and in chloroform solution. It is reasonable to attribute this to the electrostatic potential of propene (Figure 2), which attracts the HCl hydrogen toward the terminal carbon.

References and Notes

(1) Toro-Labbé, A. *J. Phys. Chem. A* **1999**, *103*, 4398.

(2) Fukui, K. *Acc. Chem. Res.* **1981**, *14*, 363.

(3) Gonzalez, C.; Schlegel, H. B. *J. Phys. Chem.* **1990**, *94*, 5523.

(4) Politzer, P.; Toro-Labbé, A.; Gutiérrez-Oliva, S.; Herrera, B.; Jaque, P.; Concha, M. C.; Murray, J. S. *J. Chem. Sci.* **2005**, *117*, 467.

(5) Toro-Labbé, A.; Gutiérrez-Oliva, S.; Murray, J. S.; Politzer, P. *Mol. Phys.* **2007**, *105*, 2619.

(6) Toro-Labbé, A.; Gutiérrez-Oliva, S.; Politzer, P.; Murray, J. S. In *Theory of Chemical Reactivity*; Chattaraj, P, Ed.; Taylor-Francis: Boca Raton, FL, 2008; Chapter 21.

(7) Jaque, P.; Toro-Labbé, A.; Politzer, P.; Geerlings, P. *Chem. Phys. Lett.* **2008**, *456*, 135.

(8) Toro-Labbé, A.; Gutiérrez-Oliva, S.; Murray, J. S.; Politzer, P. *J. Mol. Model.* **2009**, *15*, 707.

(9) Politzer, P.; Murray, J. S. *Collect. Czech. Chem. Commun.* **2008**, *73*, 822.

(10) Murray, J. S.; Toro-Labbé, A.; Clark, T.; Politzer, P. *J. Mol. Model.* **2009**, *15*, 701.

(11) Rosker, M. J.; Dantus, M.; Zewail, A. H. *J. Chem. Phys.* **1988**, *89*, 6113.

(12) Polanyi, J. C.; Zewail, A. H. *Acc. Chem. Res.* **1995**, *28*, 119.

(13) Zewail, A. H. *J. Phys. Chem. A* **2000**, *104*, 5660.

(14) Burda, J. V.; Toro-Labbé, A.; Gutiérrez-Oliva, S.; Murray, J. S.; Politzer, P. *J. Phys. Chem. A* **2007**, *111*, 2455.

(15) March, J.; *Advanced Organic Chemistry*, 3rd ed., Wiley-Interscience: New York, 1985.

(16) Klamt, A.; Schürmann, G. *J. Chem. Soc., Perkin Trans. 2* **1993**, 799.

(17) Klamt, A. *J. Phys. Chem.* **1995**, *99*, 2224.

(18) Sharp, K. A. In *Encyclopedia of Computational Chemistry*; Schleyer, P. v. R., Ed.; Wiley: New York, 1998; Vol. 1, pp 571–573.

(19) Cramer, C. J. *Essentials of Computational Chemistry*; Wiley: New York, 2002.

(20) Cossi, M.; Barone, V. *J. Phys. Chem. A* **2000**, *104*, 10614.

(21) Bader, R. F. W.; Carroll, M. T.; Cheeseman, J. R.; Chang, C. *J. Am. Chem. Soc.* **1987**, *109*, 7968.

(22) Reference for NIST database: Computational Chemistry Comparison and Benchmark Database, NIST Standard Reference Database Number 101 Release 14, Sept 2006, Editor: Russell D. Johnson III, http://srdata.nist.gov/cccbdb.